Computers in Biology and Medicine 169 (2024) 107829

Contents lists available at ScienceDirect

Computers in Biology and Medicine

journal homepage: www.elsevier.com/locate/compbiomed

Electrophysiological mechanisms underlying T wave pseudonormalisation on stress ECGs in hypertrophic cardiomyopathy

James A. Coleman [a], Ruben Doste [a], Matteo Beltrami [b], Raffaele Coppini [c], Iacopo Olivotto [b,d], Betty Raman [e,1], Alfonso Bueno-Orovio [a,*,1]

[a] Department of Computer Science, University of Oxford, Oxford, United Kingdom
[b] Cardiomyopathy Unit, Careggi University Hospital, Florence, Italy
[c] Department of NeuroFarBa, University of Florence, Florence, Italy
[d] Meyer Children's Hospital IRCCS, Florence, Italy
[e] Oxford Centre for Clinical Magnetic Resonance Research (OCMR), Radcliffe Department of Medicine, Division of Cardiovascular Medicine, University of Oxford, Oxford, United Kingdom

ARTICLE INFO

Keywords:
T wave pseudonormalisation
Stress ECG
Hypertrophic cardiomyopathy
Ischaemia
Exercise

ABSTRACT

Background: Pseudonormal T waves may be detected on stress electrocardiograms (ECGs) in hypertrophic cardiomyopathy (HCM). Either myocardial ischaemia or purely exercise-induced changes have been hypothesised to contribute to this phenomenon, but the precise electrophysiological mechanisms remain unknown.
Methods: Computational models of human HCM ventricles (n = 20) with apical and asymmetric septal hypertrophy phenotypes with variable severities of repolarisation impairment were used to investigate the effects of acute myocardial ischaemia on ECGs with T wave inversions at baseline. Virtual 12-lead ECGs were derived from a total of 520 biventricular simulations, for cases with regionally ischaemic K^+ accumulation in hypertrophied segments, global exercise-induced serum K^+ increases, and/or increased pacing frequency, to analyse effects on ECG biomarkers including ST segments, T wave amplitudes, and QT intervals.
Results: Regional ischaemic K^+ accumulation had a greater impact on T wave pseudonormalisation than exercise-induced serum K^+ increases, due to larger reductions in repolarisation gradients. Increases in serum K^+ and pacing rate partially corrected T waves in some anatomical and electrophysiological phenotypes. T wave morphology was more sensitive than ST segment elevation to regional K^+ increases, suggesting that T wave pseudonormalisation may sometimes be an early, or the only, ECG feature of myocardial ischaemia in HCM.
Conclusions: Ischaemia-induced T wave pseudonormalisation can occur on stress ECG testing in HCM before significant ST segment changes. Some anatomical and electrophysiological phenotypes may enable T wave pseudonormalisation due to exercise-induced increased serum K^+ and pacing rate. Consideration of dynamic T wave abnormalities could improve the detection of myocardial ischaemia in HCM.

1. Introduction

Hypertrophic cardiomyopathy (HCM) is the most common genetic heart disease and a leading cause of sudden cardiac death (SCD) in the young [1], with most SCDs being unpredicted. Acute myocardial ischaemia, largely subtended by microvascular and mitochondrial dysfunction, is a key contributor to lethal arrhythmias in HCM [2–4]. However, the assessment of ischaemia is yet to be included in HCM clinical guidelines or SCD risk stratification [5]. As electrophysiological changes precede lethal ischaemia-induced arrhythmias [2,6], stress electrocardiogram (ECG) testing is potentially a useful tool to identify clinically significant inducible ischaemia in HCM [7]. However, at present, stress ECG testing is considered poorly sensitive for ischaemia detection in HCM, due to significant repolarisation abnormalities on resting ECGs [8].

Repolarisation abnormalities, which are the most common finding on resting HCM ECGs, frequently involve negative T waves, ST segment depression, and prolonged QT interval [9]. These are in part attributed to heterogeneous electrophysiological remodelling in the HCM ventricles [10,11]. During exercise, repolarisation abnormalities can also

* Corresponding author.
E-mail address: alfonso.bueno@cs.ox.ac.uk (A. Bueno-Orovio).
[1] Joint senior authors.

https://doi.org/10.1016/j.compbiomed.2023.107829
Received 23 August 2023; Received in revised form 9 November 2023; Accepted 4 December 2023
Available online 7 December 2023

develop in HCM, including T wave inversion, uprighting of negative T waves (pseudonormal T waves), and worsening of baseline ST segment depression [12]. Non-specific changes during stress ECG testing have limited prognostic value in HCM [13], thus it is important to discern pathological ischaemic changes from benign changes that occur with exercise.

T wave pseudonormalisation (Fig. 1) can occur on stress ECGs in HCM [12] and is of controversial clinical significance [14]. Despite reported associations with transmural myocardial ischaemia in coronary artery disease cohorts [15], the mechanisms underlying T wave pseudonormalisation are unknown in HCM. Notably, perfusion defects are prevalent in HCM [4] and transmural septal infarction is sometimes identified at SCD autopsy [16]. Thus, potential markers of transmural ischaemia may be of clinical significance [17]. However, in-vivo investigations of the mechanisms underlying T wave pseudonormalisation are challenging due to the difficulty of performing invasive mapping protocols in these patients, and major gaps in knowledge remain.

We therefore used a human multiscale modelling and simulation approach to investigate the electrophysiological mechanisms by which T wave pseudonormalisation occurs on stress ECGs in HCM patients, and to contribute to the discussion on the clinical significance of this phenomenon. The hypothesis is that T wave pseudonormalisation occurs primarily in HCM due to an accentuated repolarisation response of the remodelled myocardium to ischaemic effects such as regional K^+ accumulation, while exercise-induced increases in serum K^+ and pacing frequency contribute to this phenomenon in a lesser extent. Therefore, to test these hypotheses, ECGs were derived from electrophysiology simulations of biventricular HCM models subjected to ischaemic regional K^+ increases, serum K^+ increases and fast pacing rates.

2. Methods

2.1. Construction of human biventricular HCM models

Representative human biventricular models of septal and apical HCM were constructed, as stress T wave pseudonormalisation has been reported in both septal obstructive [12] and apical HCM patients [18,19]. Anatomical ventricular reconstructions were therefore derived from two HCM patients: one with asymmetric septal hypertrophy, and one with apical hypertrophy.

Cardiac electrophysiology in these human biventricular models was simulated using the ToR-ORd action potential (AP) model, a biophysically detailed state-of-the-art model of human ventricular cardiomyocyte electrophysiology previously validated for HCM investigations [20,21]. Resting repolarisation abnormalities on HCM ECGs can occur due to impaired cellular repolarisation [11], secondary to remodelling in ion channels (primarily upregulation of late Na^+ and down-regulation of K^+ channels), as characterised in-vitro in surgical myectomy samples [10]. This experimentally-reported HCM ionic remodelling pattern was introduced in the virtual models by remodelling ion channel conductances (Supplementary Table S1), as in previous works [21,22]. The exact distribution of ionic remodelling in HCM ventricles is unknown, however it is thought to be most severe in hypertrophied segments, as reflected by associations between JTc dispersion and LV wall thickness heterogeneity [23]. The ionic remodelling being a downstream effect of hypertrophy is also consistent with the remodelling in myectomy samples being mutation-independent [10]. Gradients of HCM electrophysiological remodelling were therefore identically applied to the endocardial surfaces of the hypertrophied regions in both the septal and apical HCM hypertrophy models, with the affected region defined by the intersection of a 4 cm diameter sphere with the mesh. To characterise inter-subject variability in T wave pseudonormalisation, human HCM biventricular simulations were repeated for 10 human AP models selected from a larger population of AP models [22]. 10 HCM-remodelled APs were selected to have AP duration at 90 % of repolarisation (APD_{90}) in the range [420, 600] ms as reported experimentally [10], varied in 20 ms increments to consider a range of electrophysiological disease severity.

Biventricular pacing used a human physiological activation sequence as defined in previous work [11,24], and basic cycle lengths in [1000, 700, 600, 500, 400] ms were investigated. Anisotropic myocardial conduction was also modelled, with fibre, sheet and normal directions defined as in previous biventricular modelling [11]. Conductivities of $\sigma_{longitudinal} = 2.52$ mS/cm and $\sigma_{transverse} = \sigma_{transmural} = 1.57$ mS/cm were used, corresponding to myocardial conduction velocities of 60 cm/s and 40 cm/s respectively, in line with experimental measurements in humans [25,26]. Apex-to-base gradients in APD were introduced by rescaling the maximal I_{Ks} conductance for each mesh element by an (exponential) scaling factor in distance from a point defined at the apex, in the range 0.2–5 [11]. The maximal I_{Ks} conductance scaling factor was smallest at the base (0.2 ×) and greatest in the apex (5 ×), such as to produce shorter APDs at the apex, as reported experimentally in humans [27] and as in previous biventricular modelling [11]. Transmural gradients in APD were introduced by modelling endocardial and epicardial cell types as defined in the ToR-ORd model [20]. The inner 70 % of transmural width was defined as endocardial and the outer 30 % as epicardial cells, as in previous biventricular modelling [28], where the derived ECGs had T waves of appropriate polarity, magnitude, and duration. All simulations were performed using the MonoAlg3D cardiac electrophysiology simulator [29] coupled to the ToR-ORd human ventricular AP model [20] and used a spatial discretisation of 500 μm.

2.2. Modelling effects of regional and serum K^+ concentration

Regional acute myocardial ischaemic K^+ increases were modelled in the human biventricular simulations including the (i) core ischaemic zone, (ii) lateral border zone and (iii) endocardial border zone [30]. Regions affected by ischaemic K^+ increases were modelled as spherical with a diameter of 5 cm (including core and border zones) [30,31], consistent with reported concentric perfusion defects in HCM [32], which are frequently >3 cm in extent [33]. The region affected by ischaemia in the biventricular models was chosen to engulf the most hypertrophied region associated with the greatest electrophysiological remodelling, as this configuration was hypothesised to be most likely to cause T wave pseudonormalisation. Regionally ischaemic K^+ increases were therefore included in the region of septal hypertrophy in septal HCM models, and in the region of apical hypertrophy in the apical HCM models. Indeed, septal and apical infarctions have been reported in HCM

Fig. 1. Stress ECG T wave pseudonormalisation in HCM. At rest, a 53 year old man with HCM presents with an inverted T wave in V6 (left). During cardiopulmonary exercise testing (central and right panels), T wave polarity is corrected.

[34,35], and perfusion defects are more prevalent in hypertrophied segments [36]. Serum K^+ increases such as those during exercise were modelled by affecting the entire human HCM biventricular myocardium identically in septal and apical HCM models [37]. The effects of regional and serum K^+ concentrations were investigated for $[K^+]$ in 4–9 mM, consistent with healthy K^+ ranges and those estimated to occur during phase 1A of human cardiac ischaemia [38,39].

2.3. ECG analysis

ECGs were computed for each human HCM biventricular simulation using the built-in MonoAlg3D ECG solver. The standard 12-lead ECG was computed, where virtual electrodes were placed on the surface of CMR-derived torso meshes as in previous work [11]. The following ECG biomarkers were computed for each lead: the QT interval, amplitudes of inverted T wave components and the ST segment change from baseline. Baseline was considered to be with $[K^+]$ of 5 mM at 1 Hz pacing.

3. Results

3.1. Septal and apical hypertrophic cardiomyopathy phenotype models

The 10 human ventricular electrophysiological profiles used in biventricular simulations are shown in Fig. 2A, where HCM electrophysiological remodelling was characterised by significant AP prolongation. This resulted in prolonged max QT interval under baseline conditions proportional to the degree of electrophysiological remodelling (Fig. 2B), when regional remodelling was included in the septal (Fig. 2C) and apical (Fig. 2D) human biventricular HCM models. The gradients of HCM ionic remodelling correspond to a linear gradient in rescaled ionic conductances from the baseline AP model up to the maximally remodelled tissue, which corresponds to the rescaling of ionic conductances listed in Supplementary Table 1. The regionally impaired repolarisation caused heterogeneous repolarisation times in the septal (Fig. 2E) and apical (Fig. 2F) models. These repolarisation gradients manifested as morphological T wave abnormalities, which were less widespread among leads in simulations of the septal

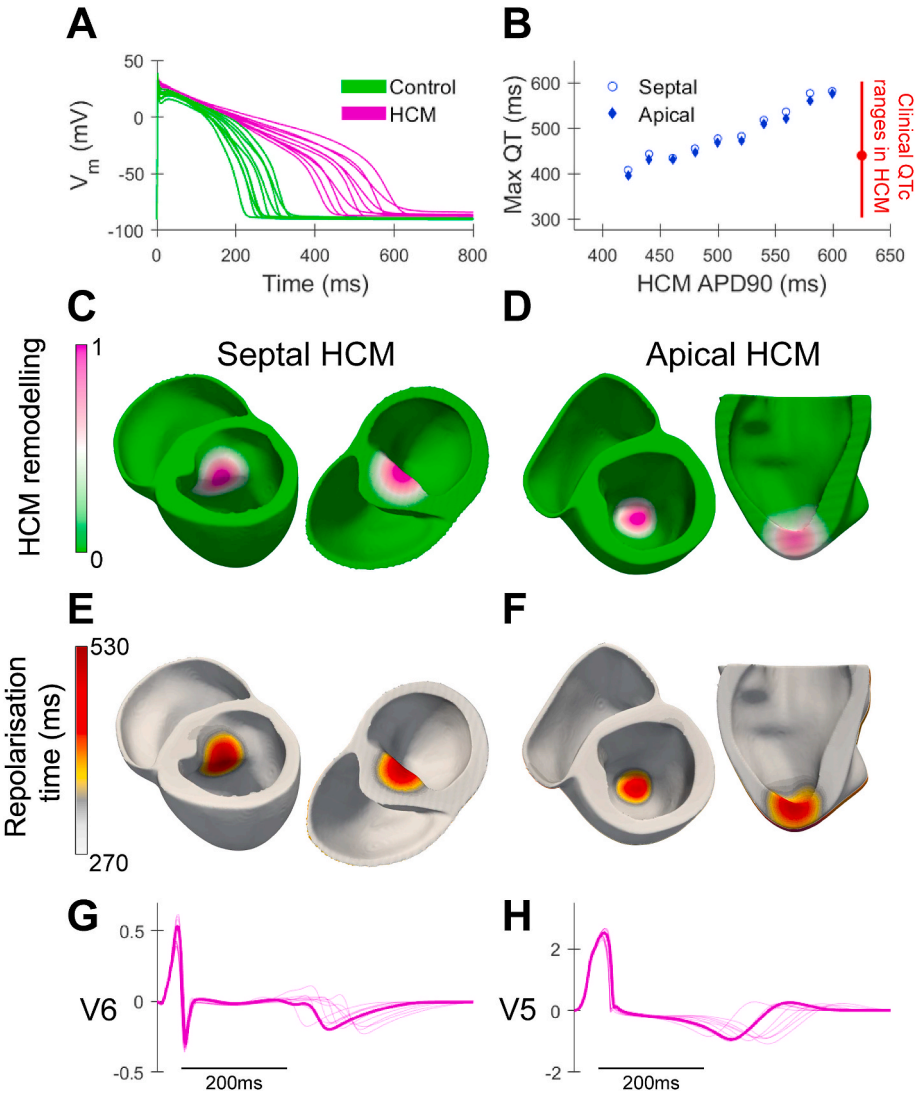

Fig. 2. Construction of septal and apical human HCM biventricular models. (A) Cellular AP traces for the 10 electrophysiological profiles used in biventricular simulations, where each human control AP model is paired with its HCM-remodelled counterpart. (B) Maximum QT interval measured from ECGs derived from the biventricular simulations against the cellular AP duration of each respective biventricular simulation, compared to clinical QT_c ranges in HCM [41]. (C, D) Distribution of HCM electrophysiological remodelling imposed in biventricular simulations for septal and apical HCM phenotypes, respectively. (E, F) Repolarisation time maps, reflecting the HCM electrophysiological remodelling for septal and apical phenotypes, respectively. (G, H) ECGs from biventricular HCM simulations, showing characteristic T wave inversions in V6 in septal (G), and V5 in apical (H) hypertrophy patterns. All results presented at 1 Hz pacing.

hypertrophy phenotype (4–5 affected: I, aVR, aVL, V5 and V6 as in Supplementary Fig. S1) than the apical hypertrophy phenotype (7–8 affected: I, II, III, aVR, aVL, aVF, V5 and V6 as in Supplementary Fig. S2), as reported clinically [40]. Representative T wave inversions are shown for V6 in the septal model (Fig. 2G) and for V5 in the apical model (Fig. 2H).

3.2. Effects of serum vs. regional K^+ on T wave abnormalities

Fig. 3 shows how, in septal HCM models, the effects of global serum K^+ increases (uniformly elevated K^+ throughout the entire ventricles) on the ECG were different to those arising from regionally ischaemic K^+ increases (elevated K^+ affecting only the region of septal hypertrophy and ionic remodelling). Representative lead V6 traces are shown for increases in serum K^+ (Fig. 3A) and regional K^+ (Fig. 3B), where significant changes to T wave morphology and QT interval are visible.

For mild [K^+] changes (4–7 mM), maximum QT interval was similarly decreased for both serum and regional K^+ increases (Fig. 3C & D), reflecting stark K^+-induced reductions in APD in the HCM-remodelled region in both cases (Supplementary Fig. S3). For severe [K^+] increases (8–9 mM), when induced regionally by ischaemia, the APD was reduced to that of, or less than, the APD of the normal myocardium, which prevented further QT interval shortening (Supplementary Fig. S4). The QT interval was instead determined by the rest of myocardium modelled as unaffected by HCM remodelling and ischaemia. For severe serum K^+ increases, the QT interval continued to decrease as the myocardium unaffected by HCM remodelling was now also affected by K^+-induced reductions in APD. A further discriminant

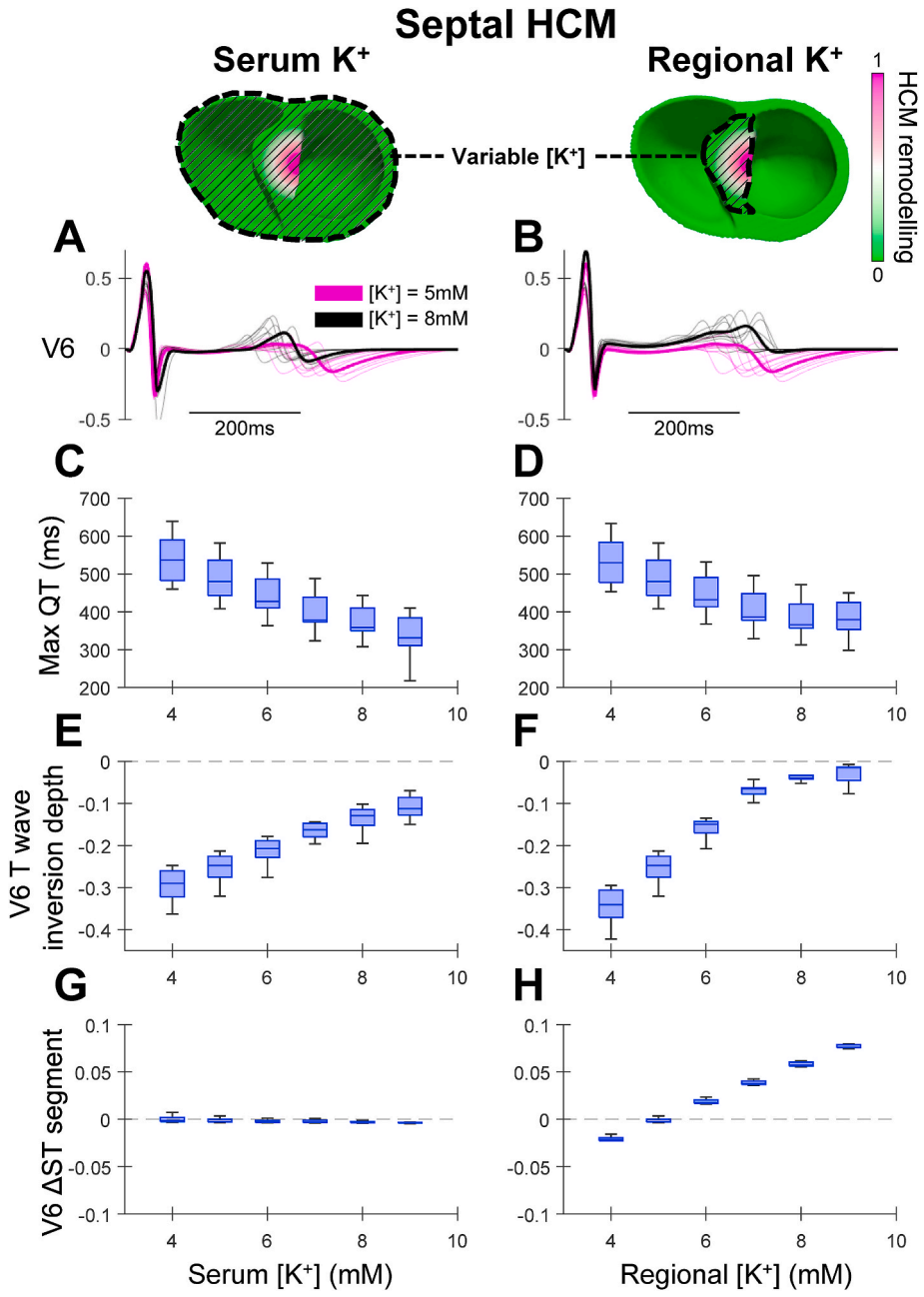

Fig. 3. Comparisons of the effect of increased serum K^+ vs. increased regional K^+ on ECG biomarkers in septal HCM. (A, B) Representative lead V6 traces, showing that T wave morphology is modulated (but not totally pseudonormalised) by serum K^+ levels (A), while full T wave pseudonormalisation can occur due to ischaemia-induced regional K^+ increases (B). (C, D) Maximum QT interval, (E, F) lead V6 T wave inversion depth, and (G, H) lead V6 ST segment changes, plotted against serum [K^+] and regional [K^+] changes, respectively. All results presented at 1 Hz pacing.

between serum and regional K^+ accumulation was that QT dispersion was decreased by regional K^+ accumulation more-so than by serum K^+ (Supplementary Fig. S5).

Differences between serum and regional K^+ increases were also observed in V6 T wave morphology (Fig. 3E & F), with ischaemia-induced regional K^+ increases causing a greater correction to T wave inversion per unit of extracellular [K^+] elevation than increases in global serum K^+. While the negative component of the T wave was almost entirely corrected in all models for elevated regional K^+ of 8–9 mM (Fig. 3F), a negative biphasic component remained in all models if subjected to serum K^+ increases (Fig. 3E).

Whereas serum K^+ did not affect the ST segment (Fig. 3G), regional K^+ increases manifested as ST elevation proportional to the degree of [K^+] increase (Fig. 3H), as is common for transmural ischaemia. In comparing Fig. 3F and H, it is notable that the magnitude of ST segment changes associated with ischaemia-induced regional K^+ increases is significantly smaller than that of changes to the T wave amplitude. This highlights that T wave pseudonormalisation may be the only perceptible ECG abnormality associated with myocardial ischaemia during stress ECG testing, particularly earlier in the onset of acute ischaemia.

When considering the other major metabolic and molecular components of acute myocardial ischaemia on top of regional K^+ accumulation, such as acidosis and activation of ATP-sensitive K^+ channels [30,31,38], pseudonormalisation of the T wave was accentuated (Supplementary Fig. S6). Furthermore, T wave pseudonormalisation occurred in proportion to the degree of colocalisation between regional K^+ accumulation and repolarisation impairment (Supplementary Fig. S7), and T wave pseudonormalisation similarly occurred when a more complex

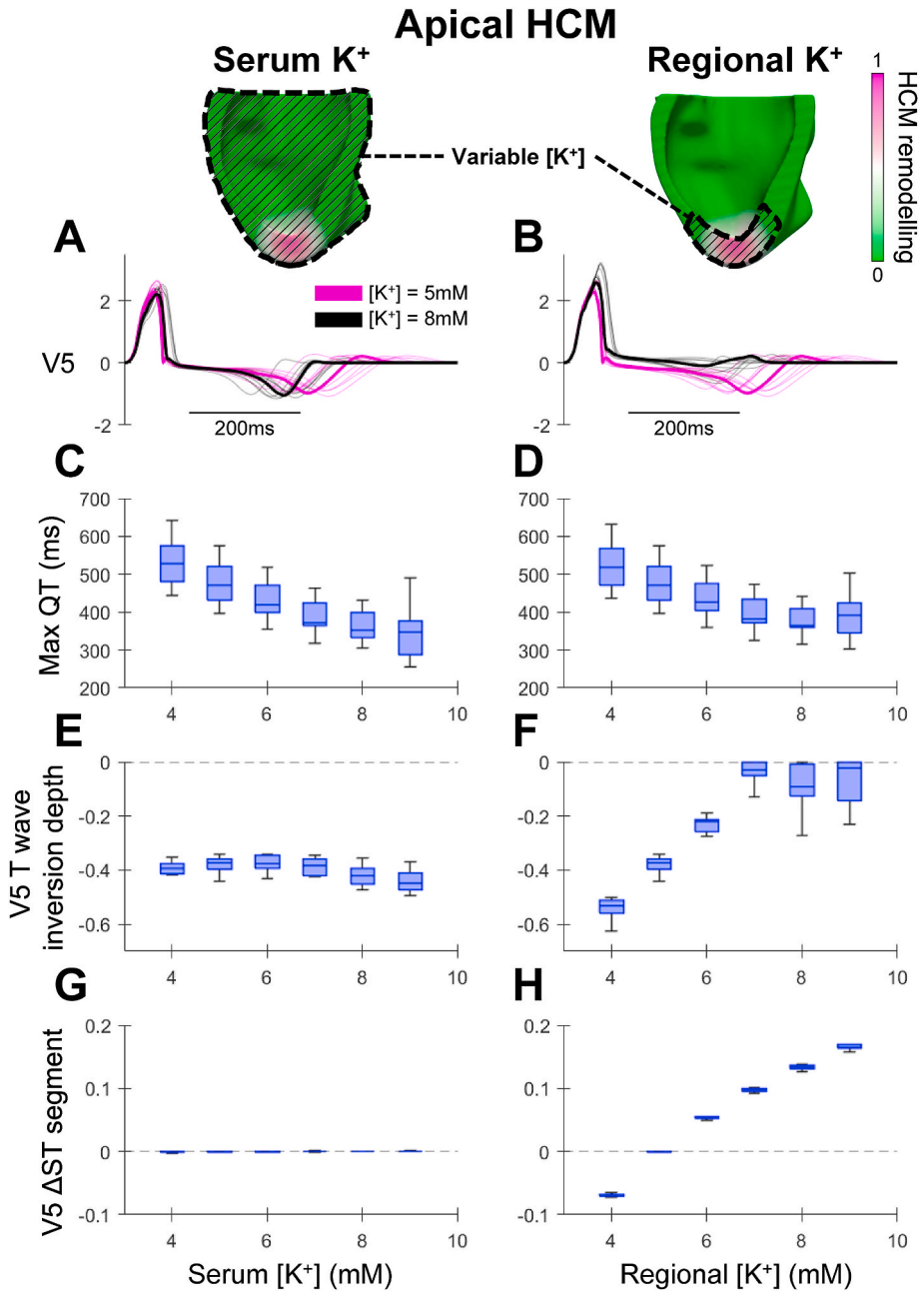

Fig. 4. Comparisons of the effect of increased serum K^+ vs. increased regional K^+ on ECG biomarkers in apical HCM. (A, B) Representative lead V5 traces, showing that T wave morphology is modulated (but not pseudonormalised) by serum K^+ (A), while full T wave pseudonormalisation can occur due to ischaemia-induced regional K^+ increases (B). (C, D) Maximum QT interval, (E, F) lead V5 T wave inversion depth, and (G, H) lead V5 ST segment changes, plotted against serum [K^+] and regional [K^+] changes, respectively. All results presented at 1 Hz pacing.

regional distribution of K^+ was considered (Supplementary Fig. S8).

Of interest, at the largest extent of global serum K^+ concentrations tested ($[K^+] = 9$ mM), some models in our virtual cohort exhibited impaired conduction and the propagation of severely stunted APs (Supplementary Fig. S9). The regions with stunted APs propagated slowly and more heterogeneously (leading to stark QRS prolongation), alongside rapid repolarisation (as stunted APs did not reach full depolarisation). Consequently, T wave peak amplitudes and terminal points were not easily discernible, and such instances were excluded from the analysis of T wave inversion. This occurred because at $[K^+] = 9$ mM, resting membrane potentials of (-74.9 ± 0.2)mV were significantly less negative than at basal conditions of (-90.0 ± 0.4)mV, which constrained fast Na^+ current availability during the AP upstroke phase. Indeed, models without discernible T waves were characterised by lower fast Na^+ channel maximal conductances of (9.1 ± 2.5)ms/μF, vs. (14.5 ± 0.7)ms/μF in models with discernible T waves. The aforementioned effects were also responsible for the increased range of maximum QT intervals observed with increasing $[K^+] = 8$ mM to $[K^+] = 9$ mM (310–440 ms vs. 220–410 ms respectively) in the remaining virtual models (Fig. 3C).

Overall, a similar behaviour was observed for HCM apical models (Fig. 4) in the dependence of QT interval and ST segment elevation on global serum K^+ increases (uniformly elevated K^+ throughout the entire ventricles) and regionally ischaemic K^+ increases (elevated K^+ affecting only the region of apical hypertrophy and ionic remodelling). However, while T wave inversion was slightly corrected by global serum K^+ increases in septal HCM models (Fig. 3E), serum K^+ increases left T wave inversions largely unaffected in apical HCM models (Fig. 4E).

The increased capacity for ischaemia-induced regional K^+ accumulation to cause T wave pseudonormalisation compared to exercise-induced global serum K^+ increases is explained in Fig. 5. Under basal conditions, T wave inversions manifest due to repolarisation gradients,

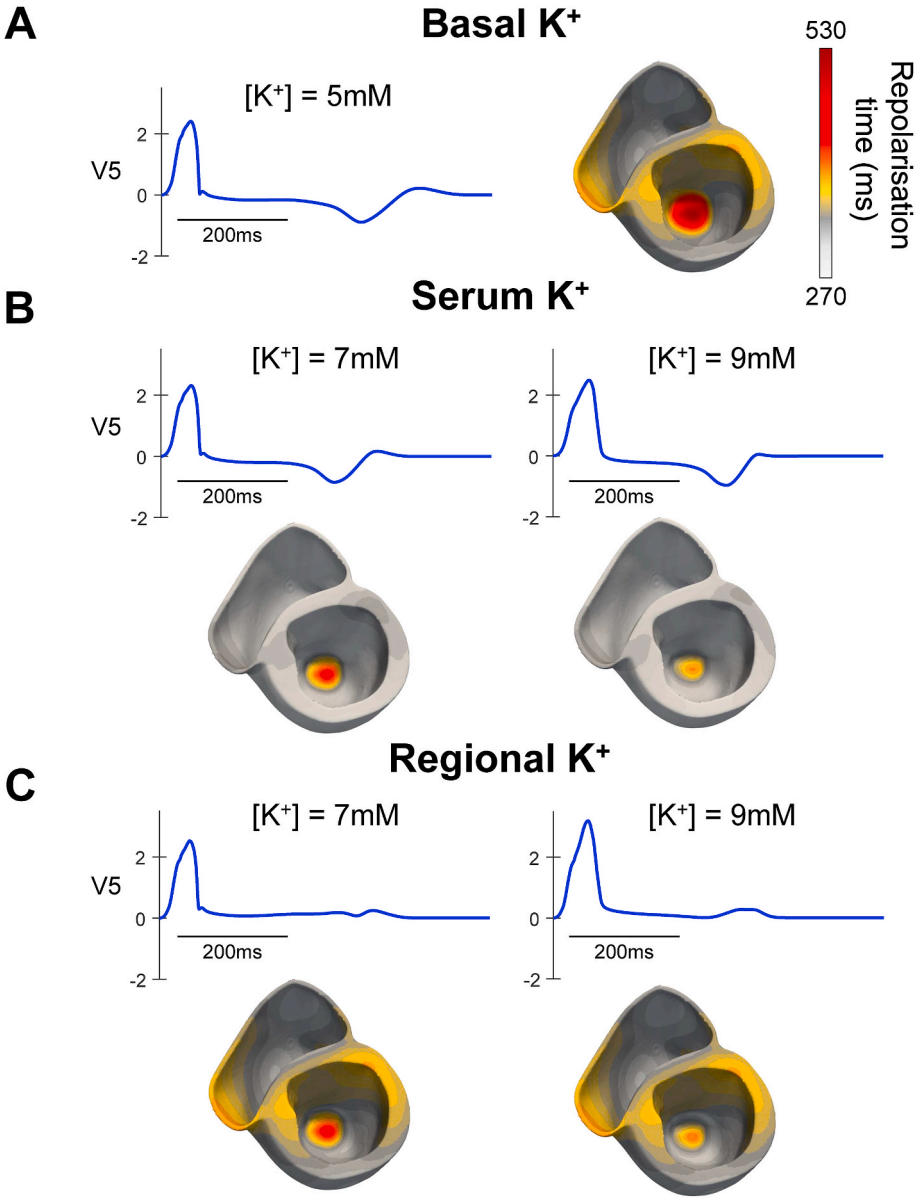

Fig. 5. Mechanism for T wave pseudonormalisation preferentially occurring due to ischaemia-induced regional K^+ accumulation vs. exercise-induced global serum K^+ elevation. (A) Under basal K^+ conditions, lead V5 T wave inversion (left), characteristic of apical HCM, occurs due to apico-basal repolarisation gradients (right). (B) During serum K^+ increases, T wave inversions persist because APs are shortened in both the region of HCM remodelling and the remote myocardium, preserving apico-basal repolarisation gradients. (C) During regional K^+ increases, T waves can become pseudonormalised because APs are shortened only in the region of HCM remodelling, correcting abnormal baseline repolarisation gradients.

caused by prolonged repolarisation in the region of hypertrophy (Fig. 5A). As serum K^+ is elevated, repolarisation times in the hypertrophic remodelled region are reduced, but repolarisation in remote myocardial regions is also accelerated, such that repolarisation gradients persist (Fig. 5B). When K^+ increase is confined to the HCM-remodelled region, the regionally prolonged repolarisation time is reduced without affecting much of the remote myocardium, such that the baseline repolarisation gradients are counteracted, leading to T wave pseudonormalisation (Fig. 5C). It is also of note that the upper range of serum K^+ considered corresponds to global cardiac ischaemia [38,39] while only a much lesser serum K^+ increase typically occurs during exercise [37], thus further minimising the possibility of ascribing T wave pseudonormalisation effects to exercise-induced increases in serum K^+.

When septal and apical models had multiple concurrent regions of K^+ elevation, T wave pseudonormalisation occurred similarly as in the case of a single region (Supplementary Figs. S10 and S11), but the second region of K^+ elevation made secondary contributions such as enhanced ST segment elevation (Supplementary Fig. S12) or new T wave notching in other leads (Supplementary Fig. S13). Finally, similar T wave pseudonormalisation occurred when finer spatial discretisations were used (Supplementary Fig. S14).

3.3. Effects of pacing rate vs. regional K^+ on T wave abnormalities

Comparisons between the effects of increased pacing rate and regionally ischaemic K^+ accumulation on the ECG are shown in Fig. 6 for septal HCM models in our virtual cohort. For both increased pacing rate and regional K^+ increases, significant changes to T wave morphology and QT interval are visible (Fig. 6A and B).

Substantial reductions to the maximum QT interval occurred at increased pacing rates due to APD rate dependence (Fig. 6C). The maximum QT interval continued to decrease at high pacing rates, contrary to the levelling off behaviour seen for high regional K^+ (Fig. 6D), for the same reasons as with the comparison to serum K^+ (APD of the HCM-remodelled region reducing to that of the APD of the non-remodelled myocardium like that shown in Supplementary Fig. S4).

Substantial but incomplete correction of T wave inversion was observed only at the highest pacing rates representative of vigorous exercise (Fig. 6E), due to enhanced APD rate-dependence of the HCM-remodelled myocardium [10], leading to partial correction of abnormal repolarisation gradients. Full T wave correction was however not observed, unlike for regional K^+ accumulation (Fig. 6F). The comparisons between serum and regional K^+ in Fig. 3 at 1 Hz were similar at 2 Hz pacing (Supplementary Fig. S15).

For the apical HCM models, as before under serum K^+ increases, increases of the pacing rate did not significantly affect T wave inversion depth (Supplementary Fig. S16).

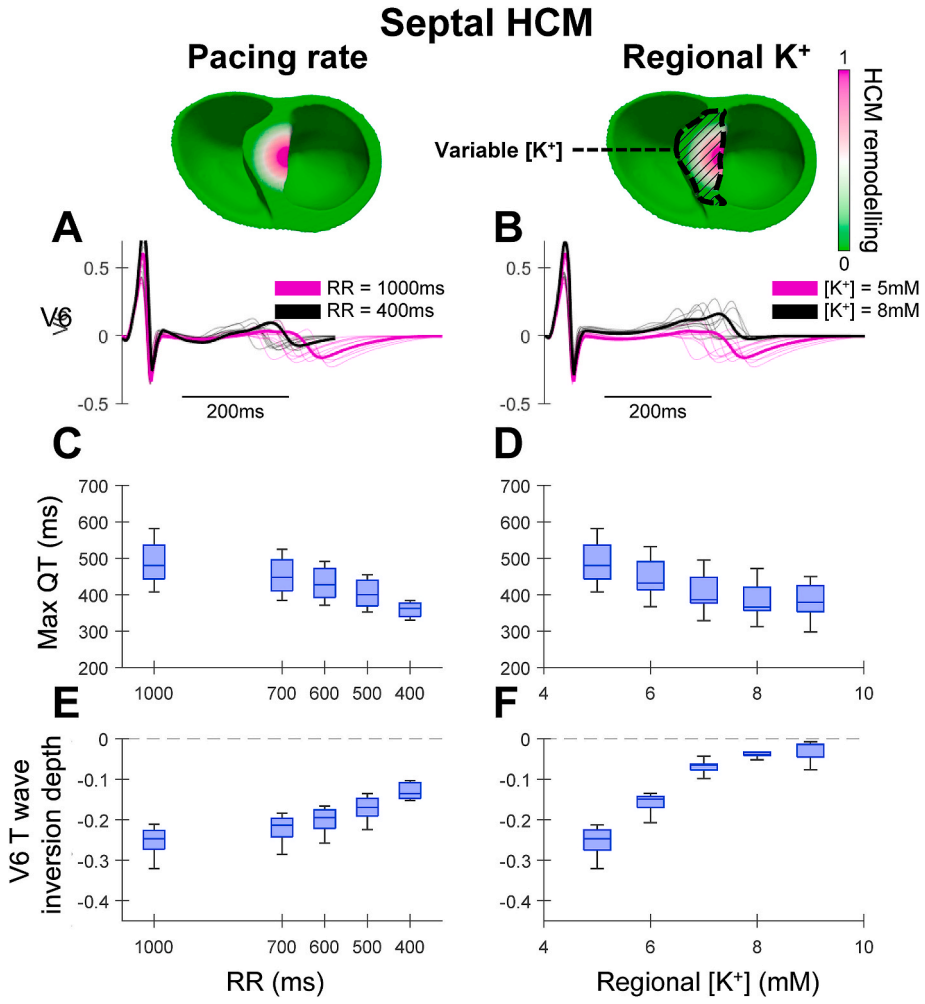

Fig. 6. Comparisons of the effects of increased pacing rate vs. regional K^+ accumulation on ECG biomarkers in septal HCM. (A, B) Representative lead V6 traces, showing that T wave morphology is modulated (but not totally pseudonormalised) by fast pacing (A), and that full T wave pseudonormalisation can occur due to regional K^+ increases (B). (C, D) Maximum QT interval, and (E, F) V6 T wave inversion depth plotted against RR interval and regional $[K^+]$, respectively.

4. Discussion

The principal findings of this study were that (i) acute regional myocardial ischaemia may frequently cause T wave pseudonormalisation in HCM if it colocalises with the remodelled myocardium; (ii) ischaemic T wave pseudonormalisation in HCM may precede or occur in the absence of significant ST segment changes; (iii) serum K^+ modulates the depth of inverted T waves, but T wave polarity is more sensitive to regional K^+ accumulation; and (iv) increased pacing rates during exercise can modulate inverted T wave amplitudes and cause partial pseudonormalisation.

The finding that acute myocardial ischaemia can normalise inverted T waves is consistent with some early reports in cohorts with high rates of ischaemic heart disease, in which deficits on perfusion imaging [15] or significant new wall motion abnormalities [42] were associated with pseudonormalisation, particularly for massive transmural deficits [43]. Similarly, severe stenosis of the left anterior descending artery has also been linked to transient T wave pseudonormalisation in apical HCM patients [19], and the frequency of stress T wave pseudonormalisation is similar to that of other markers of severe ischaemia such as ST elevation [12]. The present study suggests that this is explained by ischaemic K^+ accumulation in a sizable extent of the HCM-remodelled myocardium, which attenuates baseline repolarisation gradients in HCM and corrects T wave polarity. This is mostly consistent with the electrophysiological basis of T wave pseudonormalisation formerly hypothesised by Simon et al. [44], who speculated that it could be explained by the superposition of acute ischaemic effects on myocardial cells (AP shortening) upon chronic disease effects (AP prolongation). Our study presents computational evidence of these mechanisms, otherwise inviable to achieve in vivo in this high-risk cohort of patients. This ischaemic aetiology may also explain T wave pseudonormalisation reported in HCM during exercise [12,18] or under administration of sodium nitroprusside [45] or dobutamine [18], as exercise and pharmacologically induced vasodilation is widely reported to induce regional perfusion impairment in HCM [46]. More broadly, the findings of the present study may be related to reports that ECGs with baseline repolarisation abnormalities have a limited range in which to become more abnormal during myocardial ischaemia [47].

For T wave pseudonormalisation induced by myocardial ischaemia, these changes occur 10–30 s before frank ST elevation [43], which may be explained in the present study by the finding that T wave inversion depth was more sensitive than ST elevation to K^+ accumulation. Given that exercise-induced ischaemia may be self-limiting in HCM through dyspnoea and angina (as the genesis is due to chronic microvascular dysfunction rather than acute epicardial coronary occlusion), electrophysiological changes preceding frank ST elevation may be increasingly relevant. For example, consideration of subthreshold ST segment changes could augment the diagnosis of myocardial ischaemia if accompanied by changes in T wave polarity [43]. A further discriminant of ischaemic T wave pseudonormalisation from benign causes is that with ischaemia progression the QT interval is expected to stop decreasing, as APs in the ischaemic myocardium become shorter than those in the unaffected myocardium, such that the QT interval is dominated by the unaffected myocardium.

Stress T wave pseudonormalisation has also been reported in non-HCM patients without evidence of myocardial ischaemia [42,48]. Independent of the exact cause, it is contingent on differential APD responses between the HCM-remodelled and non-remodelled myocardium. Multiple benign causes have been hypothesised, including tachycardia-induced decreases in ventricular repolarisation gradients and sympathetic stimulation [49]. However, there is now evidence that the sympathetic response of APD in diseased HCM myocardium is abnormal, such that repolarisation gradients are likely to be enhanced under sympathetic stimulation rather than corrected [50]. Conversely, rate-dependent repolarisation gradients were shown in the present study to contribute to pseudonormalisation due to accentuated APD rate dependence in diseased HCM cells [10], consistent with the association between heart rate and T wave inversion depth observed in apical HCM [51]. As a further potential contributor, the present study investigated how the accentuated K^+ dependence in diseased HCM cells manifests as T wave changes during exercise-induced serum K^+ increases. In the scenarios tested, serum K^+ had the potential to modulate T wave inversion magnitude, but only approached pseudonormalisation during severe global hyperkalaemia. Physiological exercise serum K^+ increases alone did not lead to full T wave pseudonormalisation in the present study, but may in part explain the difficulty of diagnosing ischaemia on the ECG in HCM [8]. The enhanced dependence of repolarisation in HCM-remodelled myocardium on K^+ can lead to enhanced T wave morphological changes under benign serum K^+ increases. A further important consideration is that the T wave response to serum K^+ increases differed between the septal and apical HCM models, suggesting that there is strong dependence on the ventricular anatomy and regions affected by electrophysiological remodelling.

Altogether, these results support the hypothesis of the present study, which was that T wave pseudonormalisation may primarily be caused by regionally ischaemic K^+ accumulation in HCM, with secondary contributions from exercise-induced serum K^+ and pacing rate increases. T wave pseudonormalisation was always more sensitive to regional K^+ than serum K^+ increases, and in apical models serum K^+ or fast pacing did not correct T wave polarities, suggesting that added anatomical constraints apply to non-ischaemic T wave pseudonormalisation. The present study explains the clinically challenging diagnosis of ischaemia on stress ECG in HCM [8], as T wave changes may be multifactorial in origin, with contributions from both ischaemia and benign exercise factors. Finally, the present study motivates further investigation of subthreshold ST segment changes in combination with T wave pseudonormalisation as criteria for diagnosing ischaemia on stress ECG in HCM.

4.1. Clinical implications

The use of stress ECG testing for the diagnosis of myocardial ischaemia in HCM remains limited in accuracy due to the presence of baseline repolarisation abnormalities [8]. The present study suggests that dynamic correction of T wave polarity, as a possible manifestation of ischaemia, could improve ischaemia diagnosis in cases where ST segment changes are subthreshold. This requires further clinical study of the rates at which T wave changes are ischaemic or non-ischaemic in cause in HCM. An important implication is in the evaluation of novel pharmacological approaches for HCM. It is unknown whether myosin inhibitors (Mavacamten and Aficamten) affect inducible ischaemia in HCM, despite effects on obstruction and ECG abnormalities [53]. Similarly, a novel therapeutic approach with a mitrotrope (ninerafaxstat, akin to the anti-ischaemic drug trimetazidine) is being investigated in HCM (trial NCT04826185). In such cases, sensitive in-vivo markers of ischaemia may help understand and quantify the efficacy of these novel approaches. Finally, with the increasing use of novel machine learning approaches to identify ischaemia on the ECG [52], the present study may offer some mechanistic insight as to the performance of such algorithms.

4.2. Limitations

In the present study, the effects of K^+ concentration were explored in two configurations: regional and global. Whether there is hypertrophy-associated heterogeneity in K^+ accumulation in the ventricles accompanying exercise-induced serum K^+ increases is unknown [54]. Also, in the case of regional K^+ accumulation, ischaemia was assumed to be confined to the most hypertrophied region, but microvascular dysfunction is frequently also present in mildly hypertrophied segments. Our investigations also demonstrated that T wave pseudonormalisation is dependent on the ventricular anatomy and distribution of ionic

remodelling, so further studies may consider additional anatomical and electrophysiological HCM phenotypes. Beta-adrenergic stimulation in HCM may further constrain the ability of benign components of exercise to correct negative T waves [50]. A further consideration is that T wave inversion at baseline can also be caused by fibrosis, and the mechanisms identified in the present study would not apply to such cases. Furthermore, sudden relief of chronic disease and subsequent correction of repolarisation due to other effects, metabolic or otherwise, cannot be ruled out [45] as a cause of T wave pseudonormalisation. Finally, ECG abnormalities other than the T wave (resting ST elevation) have also been reported to normalise in some HCM patients [55].

From a computational modelling perspective, although human HCM biventricular geometries and realistic myocardial activation sequences were used, the models did not include patient-specific distributions of ischaemic K^+, myocardial disarray, Purkinje systems, mechanoelectric feedback, torsos, or atria. Finally, despite accounting for electrophysiological variability in HCM models, all simulations used the ToR-ORd AP model.

Author contributions

JAC, RD, BR and ABO developed the key ideas. JAC performed the biventricular simulations with support from RD and ABO. JAC, RD, BR and ABO drafted the original manuscript. MB, RC and BR provided clinical exercise ECGs from hypertrophic cardiomyopathy patients. MB, RC, IO and BR provided critical clinical insight and feedback. All authors contributed to revisions of the manuscript and approved the final version.

Funding

This work was supported by the UK Engineering and Physical Sciences Research Council [2421745] and the British Heart Foundation [RE/18/3/34214, FS/17/22/32644, RE/13/1/30181]. The authors acknowledge additional support from PRACE for access to Piz Daint at the Swiss National Supercomputing Centre, Switzerland (ICEI-PRACE grants icp005, icp013 and icp019), and the use of the University of Oxford Advanced Research Computing (ARC) facility (https://doi.org/10.5281/zenodo.22558). For the purpose of Open Access, the authors have applied a CC BY public copyright licence to any Author Accepted Manuscript (AAM) version arising from this submission.

Declaration of competing interest

The authors declare that they have no known competing financial interests or personal relationships that could have appeared to influence the work reported in this paper.

Appendix A. Supplementary data

Supplementary data to this article can be found online at https://doi.org/10.1016/j.compbiomed.2023.107829.

References

[1] B.J. Maron, J.J. Doerer, T.S. Haas, D.M. Tierney, F.O. Mueller, Sudden deaths in young competitive athletes, Circulation 119 (2009) 1085–1092, https://doi.org/10.1161/CIRCULATIONAHA.108.804617.

[2] E. Rochelson, L. Nappo, R.H. Pass, Hypertrophic cardiomyopathy: ischemia progressing to ventricular fibrillation, Hear Case Rep 4 (2018) 386–388, https://doi.org/10.1016/j.hrcr.2018.03.004.

[3] A. Gutiérrez Díez, A. Tamariz-Martel Moreno, A. Baño Rodrigo, A. Serrano González, Muerte súbita y fibrilación ventricular de posible origen isquémico en un niño con miocardiopatía hipertrófica, Rev. Esp. Cardiol. 53 (2000) 290–293, https://doi.org/10.1016/s0300-8932(00)75093-7.

[4] J.A. Coleman, Z. Ashkir, B. Raman, A. Bueno-Orovio, Mechanisms and prognostic impact of myocardial ischaemia in hypertrophic cardiomyopathy, Int. J. Cardiovasc. Imag. 39 (2023) 1979–1996, https://doi.org/10.1007/s10554-023-02894-y.

[5] P. Elliott, A. Anastasakis, M.A. Borger, M. Borggrefe, F. Cecchi, P. Charron, A. A. Hagege, A. Lafont, G. Limongelli, H. Mahrholdt, W.J. McKenna, J. Mogensen, P. Nihoyannopoulos, S. Nistri, P.G. Pieper, B. Pieske, C. Rapezzi, F.H. Rutten, C. Tillmanns, H. Watkins, 2014 ESC guidelines on diagnosis and management of hypertrophic cardiomyopathy: the task force for the diagnosis and management of hypertrophic cardiomyopathy of the European society of cardiology (ESC), Eur. Heart J. 35 (2014) 2733–2779, https://doi.org/10.1093/eurheartj/ehu284.

[6] J.R. Gimeno, M. Tomé-Esteban, C. Lofiego, J. Hurtado, A. Pantazis, B. Mist, P. Lambiase, W.J. McKenna, P.M. Elliott, Exercise-induced ventricular arrhythmias and risk of sudden cardiac death in patients with hypertrophic cardiomyopathy, Eur. Heart J. 30 (2009) 2599–2605, https://doi.org/10.1093/eurheartj/ehp327.

[7] J. Conway, S. Min, C. Villa, R.G. Weintraub, S. Nakano, J. Godown, M. Tatangelo, K. Armstrong, M. Richmond, B. Kaufman, A.K. Lal, S. Balaji, A. Power, N. Baez Hernandez, L. Gardin, P.F. Kantor, J.J. Parent, P.F. Aziz, J.L. Jefferies, A. Dragulescu, A. Jeewa, L. Benson, M.W. Russell, R. Whitehill, J. Rossano, T. Howard, S. Mital, The prevalence and association of exercise test abnormalities with sudden cardiac death and transplant-free survival in childhood hypertrophic cardiomyopathy, Circulation 147 (2022) 718–727, https://doi.org/10.1161/CIRCULATIONAHA.122.062699.

[8] M.S. Maron, I. Olivotto, B.J. Maron, S.K. Prasad, F. Cecchi, J.E. Udelson, P. G. Camici, The case for myocardial ischemia in hypertrophic cardiomyopathy, J. Am. Coll. Cardiol. 54 (2009) 866–875, https://doi.org/10.1016/j.jacc.2009.04.072.

[9] E. Biagini, C. Pazzi, I. Olivotto, B. Musumeci, G. Limongelli, G. Boriani, G. Pacileo, V. Mastromarino, M.L. Bacchi Reggiani, M. Lorenzini, F. Lai, A. Berardini, F. Mingardi, S. Rosmini, E. Resciniti, C. Borghi, C. Autore, F. Cecchi, C. Rapezzi, Usefulness of electrocardiographic patterns at presentation to predict long-term risk of cardiac death in patients with hypertrophic cardiomyopathy, Am. J. Cardiol. 118 (2016) 432–439, https://doi.org/10.1016/j.amjcard.2016.05.023.

[10] R. Coppini, C. Ferrantini, L. Yao, P. Fan, M. Del Lungo, F. Stillitano, L. Sartiani, B. Tosi, S. Suffredini, C. Tesi, M. Yacoub, I. Olivotto, L. Belardinelli, C. Poggesi, E. Cerbai, A. Mugelli, Late sodium current inhibition reverses electromechanical dysfunction in human hypertrophic cardiomyopathy, Circulation 127 (2013) 575–584, https://doi.org/10.1161/CIRCULATIONAHA.112.134932.

[11] A. Lyon, A. Bueno-Orovio, E. Zacur, R. Ariga, V. Grau, S. Neubauer, H. Watkins, B. Rodriguez, A. Mincholé, Electrocardiogram phenotypes in hypertrophic cardiomyopathy caused by distinct mechanisms: apico-basal repolarization gradients vs. Purkinje-myocardial coupling abnormalities, Europace 20 (2018), https://doi.org/10.1093/europace/euy226 iii102–iii112.

[12] H. Cui, H. V Schaff, T.P. Olson, J.B. Geske, J.A. Dearani, R.A. Nishimura, D. Sun, S. R. Ommen, Cardiopulmonary exercise test in patients with obstructive hypertrophic cardiomyopathy, J. Thorac. Cardiovasc. Surg. (2022), https://doi.org/10.1016/j.jtcvs.2022.05.025.

[13] Q. Ciampi, I. Olivotto, C. Gardini, F. Mori, J. Peteiro, L. Monserrat, X. Fernandez, L. Cortigiani, F. Rigo, L.R. Lopes, I. Cruz, C. Cotrim, M. Losi, S. Betocchi, B. Beleslin, M. Tesic, A.D. Dikic, E. Lazzeroni, D. Lazzeroni, R. Sicari, E. Picano, Prognostic role of stress echocardiography in hypertrophic cardiomyopathy: the International Stress Echo Registry, Int. J. Cardiol. 219 (2016) 331–338, https://doi.org/10.1016/j.ijcard.2016.06.044.

[14] S. Mishra, A. Mishra, J. Mishra, Pseudo-normalization of t-waves: review & update, Blood, Heart and Circulation 2 (2018), https://doi.org/10.15761/BHC.1000128.

[15] J.J. Marin, M.K. Heng, R. Sevrin, V.N. Udhoji, Significance of T wave normalization in the electrocardiogram during exercise stress test, Am. Heart J. 114 (1987) 1342–1348, https://doi.org/10.1016/0002-8703(87)90535-7.

[16] B.J. Maron, S.E. Epstein, W.C. Roberts, Hypertrophic cardiomyopathy and transmural myocardial infarction without significant atherosclerosis of the extramural coronary arteries, Am. J. Cardiol. 43 (1979) 1086–1102, https://doi.org/10.1016/0002-9149(79)90139-5.

[17] H. Furushima, M. Chinushi, K. Iijima, A. Sanada, D. Izumi, Y. Hosaka, Y. Aizawa, Ventricular tachyarrhythmia associated with hypertrophic cardiomyopathy: incidence, prognosis, and relation to type of hypertrophy, J. Cardiovasc. Electrophysiol. 21 (2010) 991–999, https://doi.org/10.1111/j.1540-8167.2010.01769.x.

[18] S. Kang, W.-H. Choi, Pseudonormalization of negative T wave during stress test in asymptomatic patients without ischemic heart disease: a clue to apical hypertrophic cardiomyopathy? Cardiology 124 (2013) 91–96, https://doi.org/10.1159/000346235.

[19] N. Arima, Y. Ochi, M. Takahashi, T. Moriki, T. Noguchi, T. Kubo, N. Yamasaki, H. Kitaoka, Transient decrease in the depth of the negative T wave in apical hypertrophic cardiomyopathy is a sign of left anterior descending artery stenosis: a case series, Eur Heart J Case Rep 7 (2023), https://doi.org/10.1093/ehjcr/ytad034 ytad034.

[20] J. Tomek, A. Bueno-Orovio, E. Passini, X. Zhou, A. Minchole, O. Britton, C. Bartolucci, S. Severi, A. Shrier, L. Virag, A. Varro, B. Rodriguez, Development, calibration, and validation of a novel human ventricular myocyte model in health, disease, and drug block, Elife 8 (2019), e48890, https://doi.org/10.7554/eLife.48890.

[21] R. Doste, R. Coppini, A. Bueno-Orovio, Remodelling of potassium currents underlies arrhythmic action potential prolongation under beta-adrenergic stimulation in hypertrophic cardiomyopathy, J. Mol. Cell. Cardiol. 172 (2022) 120–131, https://doi.org/10.1016/j.yjmcc.2022.08.361.

[22] E. Passini, A. Mincholé, R. Coppini, E. Cerbai, B. Rodriguez, S. Severi, A. Bueno-Orovio, Mechanisms of pro-arrhythmic abnormalities in ventricular repolarisation and anti-arrhythmic therapies in human hypertrophic cardiomyopathy, J. Mol. Cell. Cardiol. 96 (2016) 72–81, https://doi.org/10.1016/j.yjmcc.2015.09.003.

[23] K. Sakata, M. Shimizu, H. Ino, M. Yamaguchi, H. Terai, K. Hayashi, M. Kiyama, T. Hayashi, M. Inoue, H. Mabuchi, QT dispersion and left ventricular morphology in patients with hypertrophic cardiomyopathy, Heart 89 (2003) 882, https://doi.org/10.1136/heart.89.8.882.

[24] L. Cardone-Noott, A. Bueno-Orovio, A. Mincholé, N. Zemzemi, B. Rodriguez, Human ventricular activation sequence and the simulation of the electrocardiographic QRS complex and its variability in healthy and intraventricular block conditions, Europace 18 (2016), https://doi.org/10.1093/europace/euw346 iv4–iv15.

[25] P. Taggart, P.M.I. Sutton, T. Opthof, R. Coronel, R. Trimlett, W. Pugsley, P. Kallis, Inhomogeneous transmural conduction during early ischaemia in patients with coronary artery disease, J. Mol. Cell. Cardiol. 32 (2000) 621–630, https://doi.org/10.1006/jmcc.2000.1105.

[26] R. Van Dam, J.P. Roos, D. Durrer, Electrical activation of ventricles and interventricular septum in hypertrophic obstructive cardiomyopathy, Br. Heart J. 34 (1972) 100–112, https://doi.org/10.1136/hrt.34.1.100.

[27] C. Ramanathan, P. Jia, R. Ghanem, K. Ryu, Y. Rudy, Activation and repolarization of the normal heart under complete physiological conditions, Proc. Natl. Acad. Sci. U. S. A. 103 (2006) 6309–6314, https://doi.org/10.1073/pnas.0601533103.

[28] R. Coppini, C. Ferrantini, M. Pioner Josè, L. Santini, J. Wang Zhinuo, C. Palandri, M. Scardigli, G. Vitale, L. Sacconi, P. Stefàno, L. Flink, K. Riedy, S. Pavone Francesco, E. Cerbai, C. Poggesi, A. Mugelli, A. Bueno-Orovio, I. Olivotto, V. Sherrid Mark, Electrophysiological and contractile effects of disopyramide in patients with obstructive hypertrophic cardiomyopathy, J Am Coll Cardiol Basic Trans Science 4 (2019) 795–813, https://doi.org/10.1016/j.jacbts.2019.06.004.

[29] R. Sachetto Oliveira, B. Martins Rocha, D. Burgarelli, W. Meira Jr., C. Constantinides, R. Weber dos Santos, Performance evaluation of GPU parallelization, space-time adaptive algorithms, and their combination for simulating cardiac electrophysiology, Int J Numer Method Biomed Eng 34 (2018), e2913, https://doi.org/10.1002/cnm.2913.

[30] S. Dutta, A. Mincholé, E. Zacur, T.A. Quinn, P. Taggart, B. Rodriguez, Early afterdepolarizations promote transmural reentry in ischemic human ventricles with reduced repolarization reserve, Prog. Biophys. Mol. Biol. 120 (2016) 236–248, https://doi.org/10.1016/j.pbiomolbio.2016.01.008.

[31] H. Martinez-Navarro, A. Mincholé, A. Bueno-Orovio, B. Rodriguez, High arrhythmic risk in antero-septal acute myocardial ischemia is explained by increased transmural reentry occurrence, Sci. Rep. 9 (2019), 16803, https://doi.org/10.1038/s41598-019-53221-2.

[32] E.K. Kim, S.-C. Lee, S.-A. Chang, S.-Y. Jang, S.M. Kim, S.-J. Park, J.-O. Choi, S. W. Park, E.-S. Jeon, Y.H. Choe, Prevalence and clinical significance of cardiovascular magnetic resonance adenosine stress-induced myocardial perfusion defect in hypertrophic cardiomyopathy, J. Cardiovasc. Magn. Reson. 22 (2020) 30, https://doi.org/10.1186/s12968-020-00623-1.

[33] J. Takata, P.J. Counihan, J.N. Gane, Y. Doi, T. Chikamori, T. Ozawa, W. J. McKenna, Regional thallium-201 washout and myocardial hypertrophy in hypertrophic cardiomyopathy and its relation to exertional chest pain, Am. J. Cardiol. 72 (1993) 211–217, https://doi.org/10.1016/0002-9149(93)90162-6.

[34] G. Limongelli, P. Calabro', G. Pacileo, G. Santoro, R. Calabro', Myocardial infarction in a young athlete with non-obstructive hypertrophic cardiomyopathy and normal coronary arteries, Int. J. Cardiol. 115 (2007) e71–e73, https://doi.org/10.1016/j.ijcard.2006.07.206.

[35] E. Mershina, O. Blagova, V. Sinitsyn, E. Pershina, A case of hypertrophic cardiomyopathy with "burned-out" apex of the left ventricle due to mid-ventricular obstruction, Clin Case Rep Rev 2 (2016), https://doi.org/10.15761/CCRR.1000S2002.

[36] P. Garcia Brás, S. Aguiar Rosa, B. Thomas, A. Fiarresga, I. Cardoso, R. Pereira, G. Branco, I. Cruz, L. Baquero, R. Cruz Ferreira, M. Mota Carmo, L. Rocha Lopes, Associations between perfusion defects, tissue changes and myocardial deformation in hypertrophic cardiomyopathy, uncovered by a cardiac magnetic resonance segmental analysis, Rev. Port. Cardiol. 41 (2022) 559–568, https://doi.org/10.1016/j.repc.2022.03.003.

[37] J. Zoladz, K. Duda, J. Majerczak, P. Thor, Effect of different cycling frequencies during incremental exercise on the venous plasma potassium concentration in humans, Physiol. Res./Academia Scientiarum Bohemoslovaca. 51 (2002) 581–586.

[38] I. V Kazbanov, R.H. Clayton, M.P. Nash, C.P. Bradley, D.J. Paterson, M.P. Hayward, P. Taggart, A. V Panfilov, Effect of global cardiac ischemia on human ventricular fibrillation: insights from a multi-scale mechanistic model of the human heart, PLoS Comput. Biol. 10 (2014), e1003891, https://doi.org/10.1371/journal.pcbi.1003891.

[39] R.H. Clayton, M.P. Nash, C.P. Bradley, A. v Panfilov, D.J. Paterson, P. Taggart, Experiment-model interaction for analysis of epicardial activation during human ventricular fibrillation with global myocardial ischaemia, Prog. Biophys. Mol. Biol. 107 (2011) 101–111, https://doi.org/10.1016/j.pbiomolbio.2011.06.010.

[40] C.H. Park, H. Chung, Y. Kim, J.-Y. Kim, P.-K. Min, K.-A. Lee, Y.W. Yoon, T.H. Kim, B.K. Lee, B.-K. Hong, S.-J. Rim, H.M. Kwon, E.-Y. Choi, Electrocardiography based prediction of hypertrophy pattern and fibrosis amount in hypertrophic cardiomyopathy: comparative study with cardiac magnetic resonance imaging, Int. J. Cardiovasc. Imag. 34 (2018) 1619–1628, https://doi.org/10.1007/s10554-018-1365-6.

[41] J.N. Johnson, C. Grifoni, J.M. Bos, M. Saber-Ayad, S.R. Ommen, S. Nistri, F. Cecchi, I. Olivotto, M.J. Ackerman, Prevalence and clinical correlates of QT prolongation in patients with hypertrophic cardiomyopathy, Eur. Heart J. 32 (2011) 1114–1120, https://doi.org/10.1093/eurheartj/ehr021.

[42] C.J. Lavie, J.K. Oh, H.T. Mankin, I.P. Clements, E.R. Giuliani, R.J. Gibbons, Significance of T-wave pseudonormalization during exercise: a radionuclide angiographic study, Chest 94 (1988) 512–516, https://doi.org/10.1378/chest.94.3.512.

[43] A. Maseri, S. Severi, M. de Nes, A. L'Abbate, S. Chierchia, M. Marzilli, A. M. Ballestra, O. Parodi, A. Biagini, A. Distante, "Variant" angina: one aspect of a continuous spectrum of vasospastic myocardial ischemia: pathogenetic mechanisms, estimated incidence and clinical and coronary arteriographic findings in 138 patients, Am. J. Cardiol. 42 (1978) 1019–1035, https://doi.org/10.1016/0002-9149(78)90691-4.

[44] A. Simon, J. Robins, T.E.H. Hooghoudt, A. Ophuis, Pseudonormalisation of the T wave: old wine? Neth. Heart J. 15 (2007) 257–259, https://doi.org/10.1007/BF03085994.

[45] S. Trevethan, R. Castilla, G. Medrano, A. de Michelli, Giant T waves simulating apical hypertrophic myocardiopathy that disappear with sodium nitroprusside administration: case report of pheochromocytoma, J. Electrocardiol. 24 (1991) 267–275, https://doi.org/10.1016/0022-0736(91)90033-I.

[46] E. Lazzeroni, E. Picano, L. Morozzi, A.R. Maurizio, G. Palma, R. Ceriati, E. Iori, A. Barilli, Dipyridamole-induced ischemia as a prognostic marker of future adverse cardiac events in adult patients with hypertrophic cardiomyopathy, Circulation 96 (1997) 4268–4272, https://doi.org/10.1161/01.CIR.96.12.4268.

[47] A. Rubulis, J. Jensen, G. Lundahl, J. Tapanainen, L. Bergfeldt, Ischemia induces aggravation of baseline repolarization abnormalities in left ventricular hypertrophy: a deleterious interaction, J. Appl. Physiol. 101 (2006) 102–110, https://doi.org/10.1152/japplphysiol.01334.2005.

[48] H.S. Loeb, N.C. Friedman, Normalization of abnormal T-waves during stress testing does not identify patients with reversible perfusion defects, Clin. Cardiol. 30 (2007) 403–407, https://doi.org/10.1002/clc.20111.

[49] V. Aravindakshan, B. Surawicz, R.D. Allen, Electrocardiographic exercise test in patients with abnormal T waves at rest, Am. Heart J. 93 (1977) 706–714, https://doi.org/10.1016/s0002-8703(77)80065-3.

[50] R. Coppini, M. Beltrami, R. Doste, A. Bueno-Orovio, C. Ferrantini, G. Vitale, J. M. Pioner, L. Santini, A. Argirò, M. Berteotti, F. Mori, N. Marchionni, P. Stefàno, E. Cerbai, C. Poggesi, I. Olivotto, Paradoxical prolongation of QT interval during exercise in patients with hypertrophic cardiomyopathy: cellular mechanisms and implications for diastolic function, Eur. Heart J. 2 (2022), https://doi.org/10.1093/ehjopen/oeac034 oeac034.

[51] F. Ma, Y. Yang, J. Tao, X. Deng, X. Chen, J. Fan, X. Bai, T. Dai, S. Li, X. Yang, F. Lin, Twenty-four hour variability of inverted T-waves in patients with apical hypertrophic cardiomyopathy, Front Cardiovasc Med 9 (2022), https://doi.org/10.3389/fcvm.2022.1004178.

[52] G. Tison, S. Konstantinos, S. Abreau, Z. Attia, P. Agarwal, A. Balabsubramanyam, Y. Li, A. Sehnert, J. Edelberg, P. Friedman, J. Olgin, P. Noseworthy, Assessment of disease status and treatment response with artificial Intelligence−Enhanced electrocardiography in obstructive hypertrophic cardiomyopathy, J. Am. Coll. Cardiol. 79 (2022) 1032–1034, https://doi.org/10.1016/j.jacc.2022.01.005.

[53] E.M. Green, H. Wakimoto, R.L. Anderson, M.J. Evanchik, J.M. Gorham, B. C. Harrison, M. Henze, R. Kawas, J.D. Oslob, H.M. Rodriguez, Y. Song, W. Wan, L. A. Leinwand, J.A. Spudich, R.S. McDowell, J.G. Seidman, C.E. Seidman, A small-molecule inhibitor of sarcomere contractility suppresses hypertrophic cardiomyopathy in mice, Science 351 (2016) (1979) 617–621, https://doi.org/10.1126/science.aad3456.

[54] J.T. Vermeulen, H.L. Tan, H. Rademaker, C.A. Schumacher, P. Loh, T. Opthof, R. Coronel, M.J. Janse, Electrophysiologic and extracellular ionic changes during acute ischemia in failing and normal rabbit myocardium, J. Mol. Cell. Cardiol. 28 (1996) 123–131, https://doi.org/10.1006/jmcc.1996.0012.

[55] T. Kawasaki, A. Azuma, T. Kuribayashi, T. Taniguchi, N. Miyai, T. Kamitani, S. Kawasaki, H. Matsubara, H. Sugihara, Resting ST-segment depression predicts exercise-induced subendocardial ischemia in patients with hypertrophic cardiomyopathy, Int. J. Cardiol. 107 (2006) 267–274, https://doi.org/10.1016/j.ijcard.2005.03.031.